**Supporting Information**

# Electrostatic contribution to $^{19}$F chemical shifts in fluorotryptophans in proteins

Michael Maxwell,[†,#] Yi Jiun Tan,[†,#] Richmond Lee,[‡] Thomas Huber,[§] Gottfried Otting[†,*]

[†]Australian Research Council Centre of Excellence for Innovations in Peptide and Protein Science, Research School of Chemistry, Australian National University, Canberra, ACT 2601, Australia

[‡]School of Chemistry and Molecular Bioscience, University of Wollongong, Wollongong, NSW 2500, Australia

[§]Research School of Chemistry, Australian National University, Canberra, ACT 2601, Australia

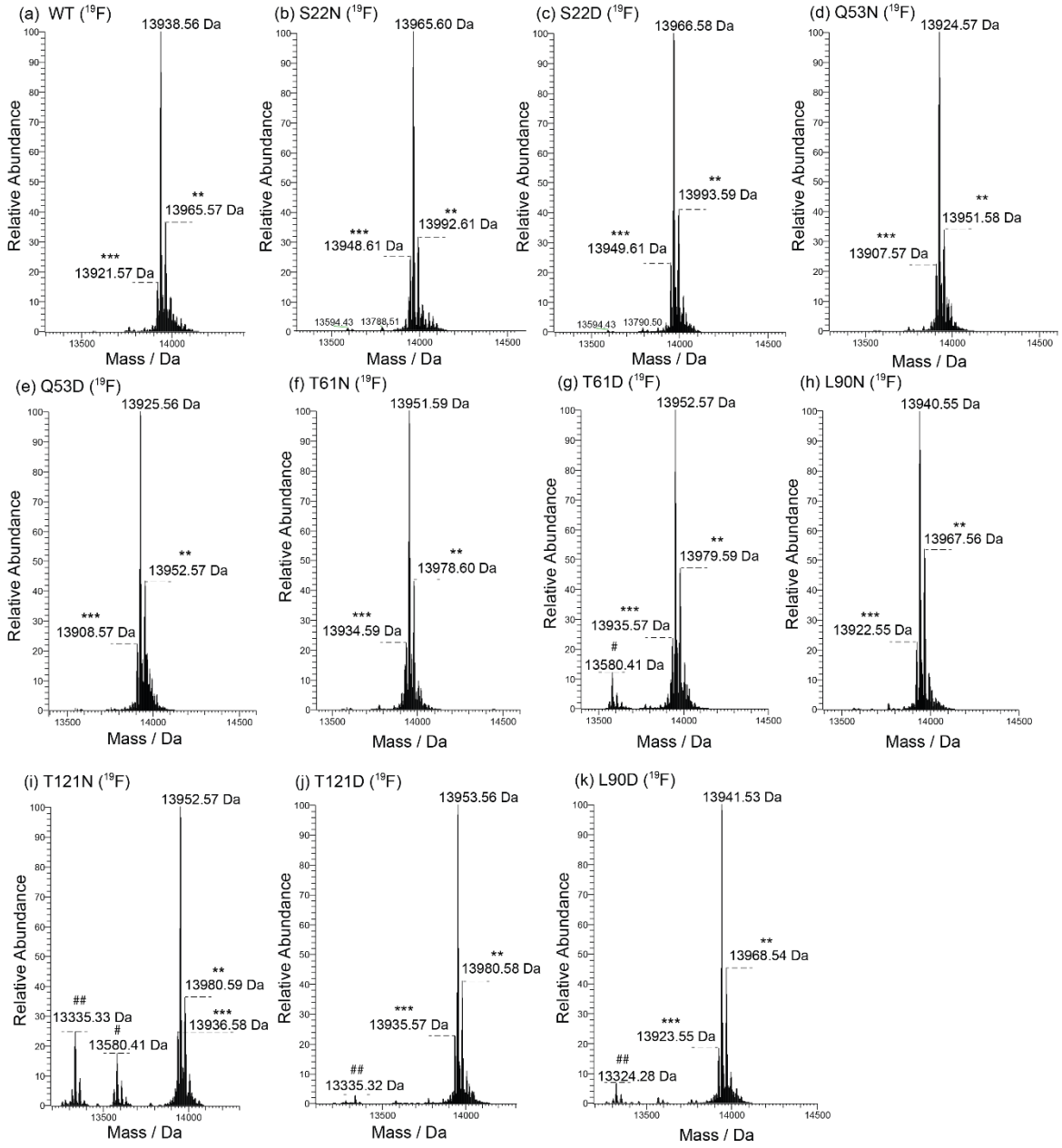


**Figure S1.** Mass spectra of NT* domain mutants showing the incorporation of fluorotryptophan. All main peaks were within 1 Da of the calculated masses. Mass peaks labeled with a star identify impurities from previous samples in the spectrometer. ** Mass attributed to formylation. Mass spectra were recorded of protein dissolved in 0.1% formic acid. *** Mass peak with tryptophan instead of fluorotryptophan. # Mass arising from C-terminal truncation (without the peptide DVSA). ## Mass arising from C-terminal truncation (without the peptide MNDVSA). (a) NT* domain WT, (b) NT* S22N mutant, (c) NT* S22D mutant, (d) NT* Q53N mutant, (e) NT* Q53D mutant, (f) NT* T61N mutant, (g) NT* T61D mutant, (h) NT* L90N mutant, (i) NT* T121N mutant, (j) NT* T121D mutant, (k) NT* L90D mutant.

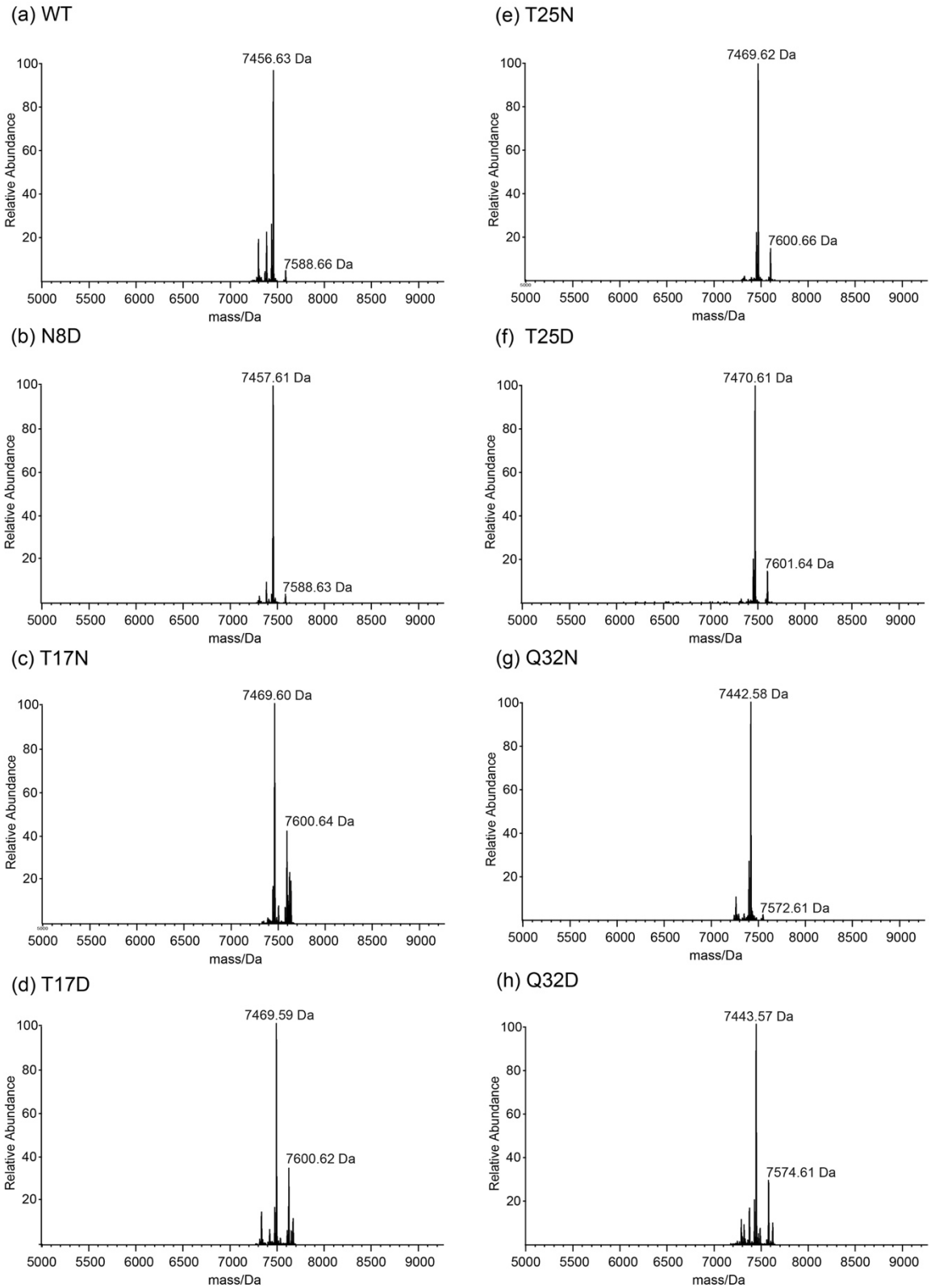
(a) WT
7456.63 Da
7588.66 Da
(e) T25N
7469.62 Da
7600.66 Da
(b) N8D
7457.61 Da
7588.63 Da
(f) T25D
7470.61 Da
7601.64 Da
(c) T17N
7469.60 Da
7600.64 Da
(g) Q32N
7442.58 Da
7572.61 Da
(d) T17D
7469.59 Da
7600.62 Da
(h) Q32D
7443.57 Da
7574.61 Da
Relative Abundance
mass/Da

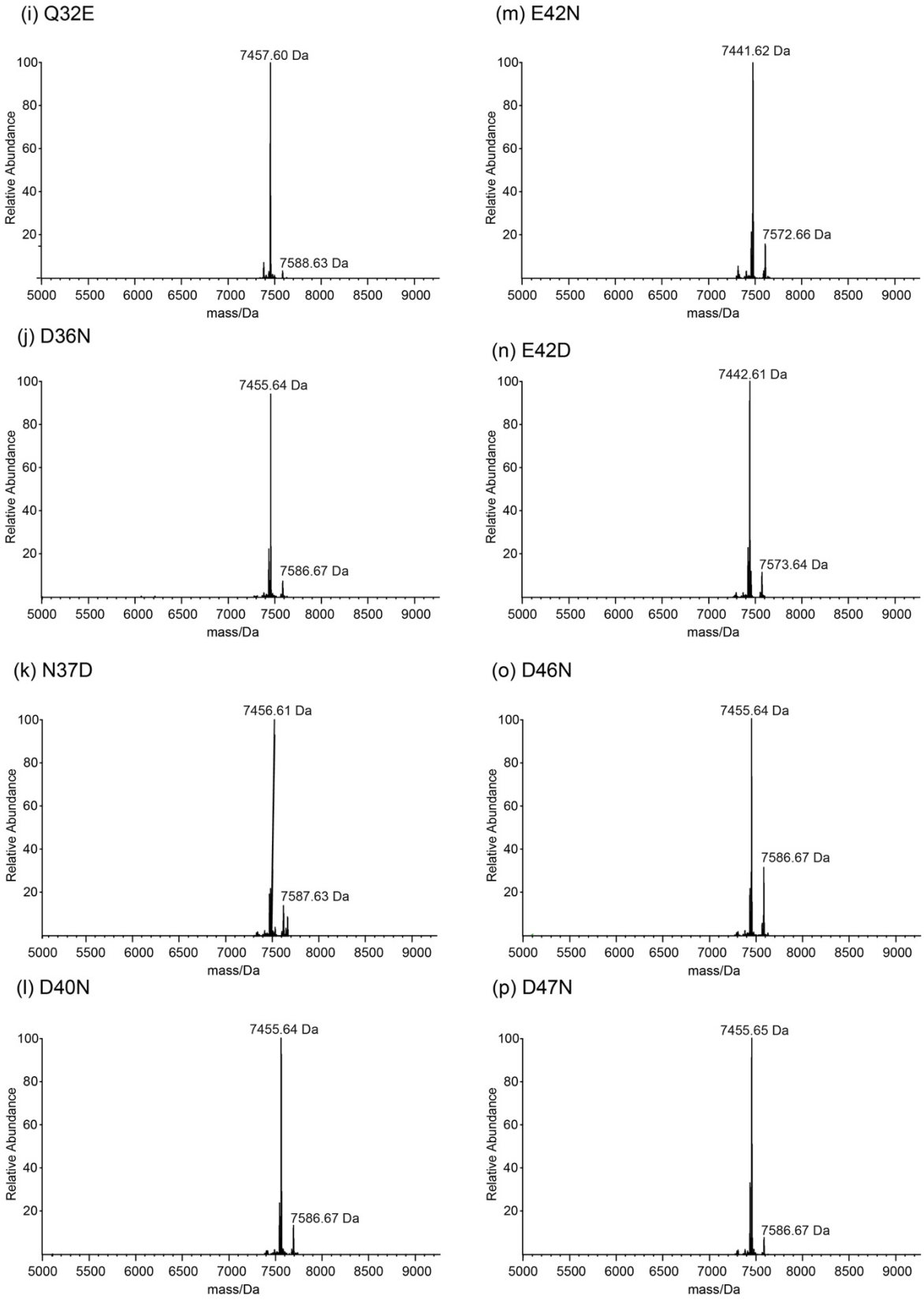


**Figure S2.** Mass spectra of different GB1 mutants made with fluorotryptophan. The main peaks are from protein without the N-terminal methionine. Minor mass peaks displaced by 131.2 Da correspond to protein including the N-terminal methionine. (a) GB1 WT, (b) GB1

N8D mutant, (c) GB1 T17N mutant, (d) GB1 T17D mutant, (e) GB1 T25N mutant, (f) GB1 T25D mutant, (g) GB1 Q32N mutant, (h) GB1 Q32D mutant, (i) GB1 Q32E mutant, (j) GB1 D36N mutant, (k) GB1 N37D mutant, (l) GB1 D40N mutant, (m) GB1 E42N mutant, (n) GB1 E42D mutant, (o) GB1 D46N mutant, (p) GB1 D47N mutant.

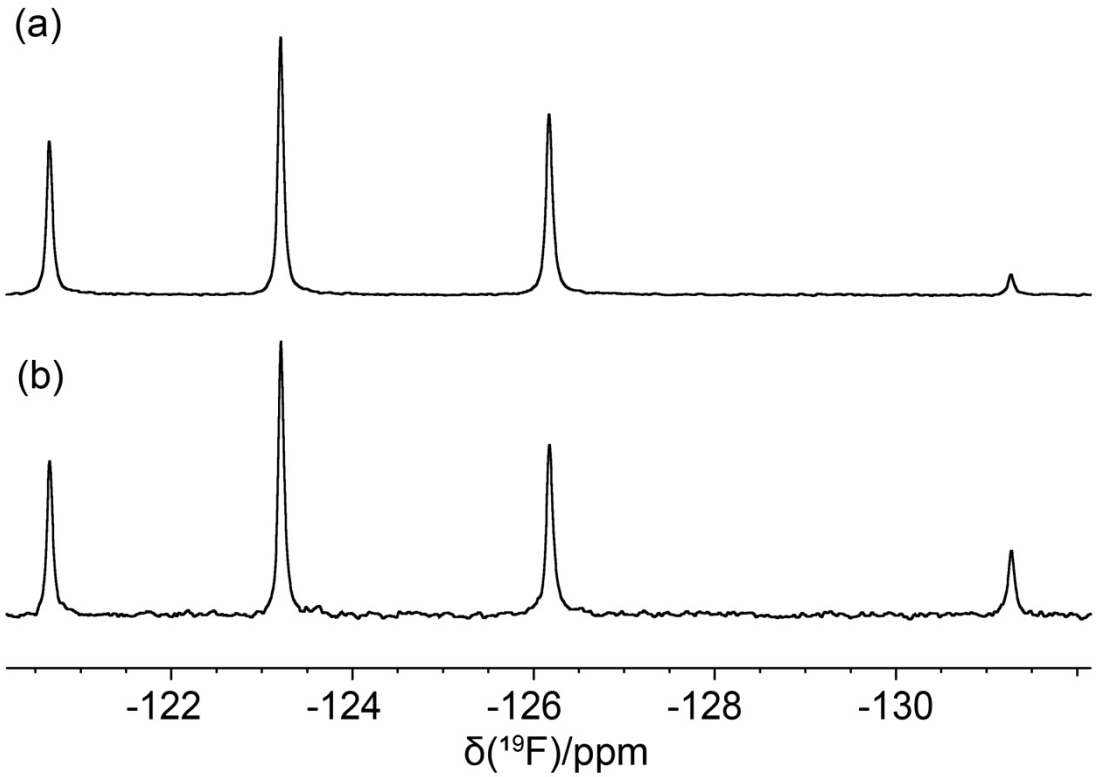


**Figure S3.** $^{19}F$ NMR spectra of wild-type GB1 made with mixtures of 4-, 5-, 6-, and 7-fluoroindole. The spectra were measured without $^{1}H$ decoupling. The full line widths at half height are 25±1 Hz. (a) Sample made by CFPS with 1 mM concentration of each of the four fluoroindoles. The relative signal integrals (low-field to high-field) are 8:12:10:1. (b) Same as (a) but using a final concentration of 1 mM 4-, 5-, 6-fluoroindole and 4 mM 7-fluoroindole.

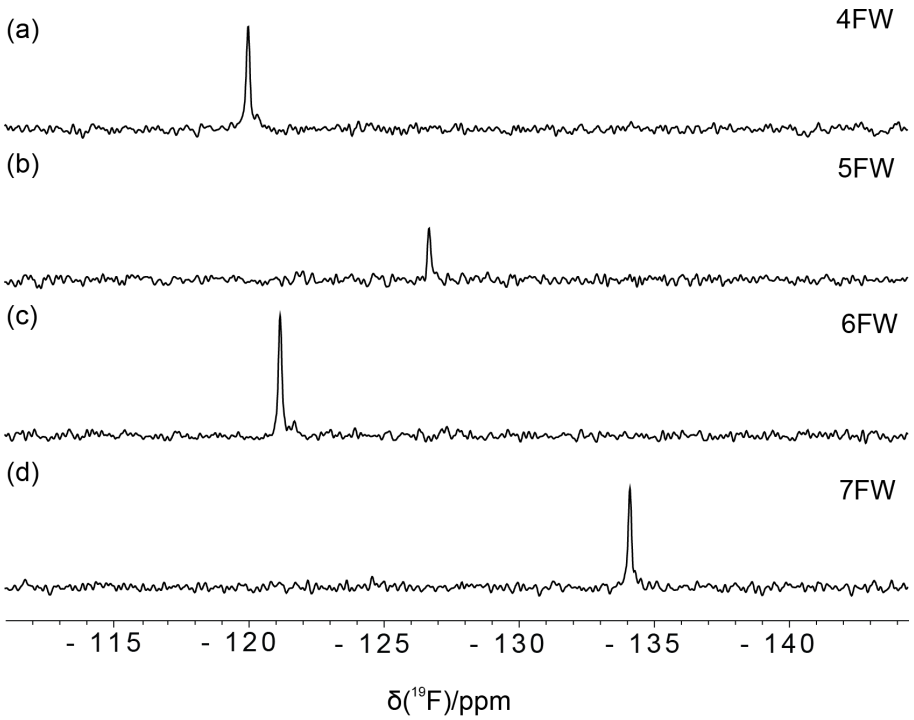


**Figure S4.** 1D $^{19}$F NMR spectra of NT* domain with different individual fluorotryptophans. (a) 4FW, (b) 5FW, (c) 6FW, (d) 7FW.

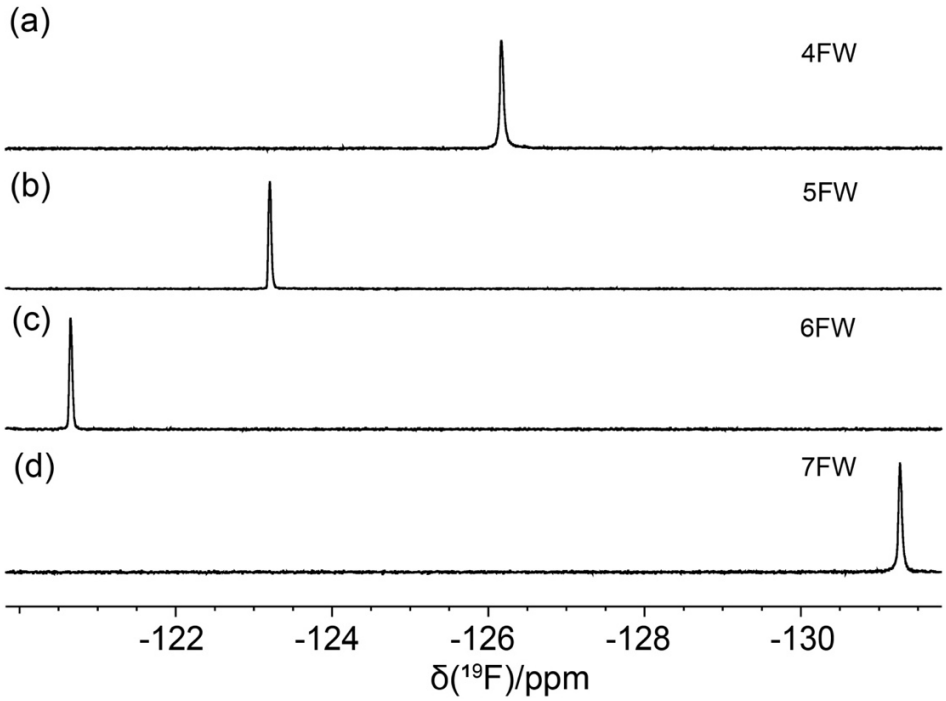


**Figure S5.** 1D $^{19}$F NMR spectra of GB1 with different individual fluorotryptophans. (a) 4FW, (b) 5FW, (c) 6FW, (d) 7FW.

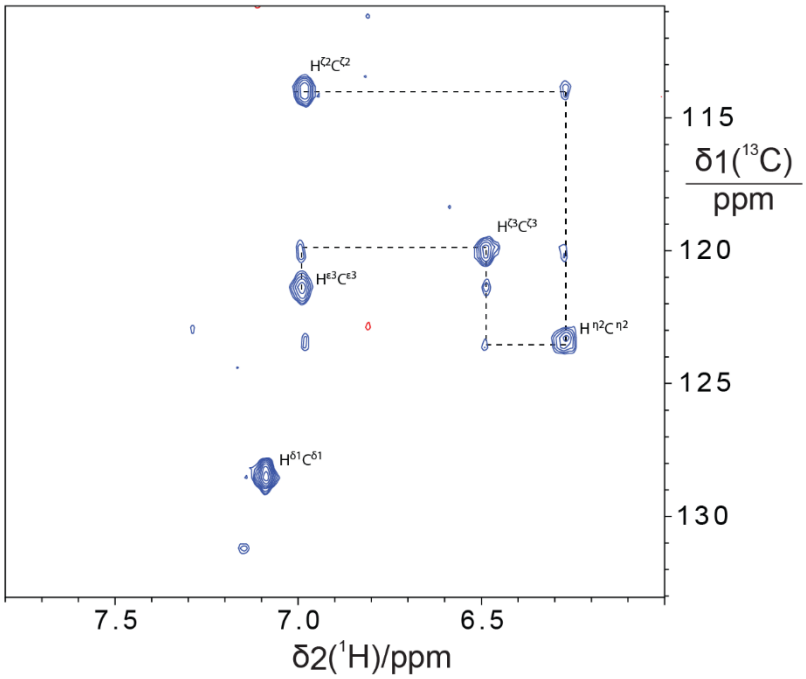


**Figure S6.** $^{13}$C-HSQC with TOCSY relay (20 ms mixing time) for the assignment of the tryptophan indole protons in the NT* domain. The cross-peaks link the 4, 5, 6, and 7 positions (ε3, ζ3, η2, ζ2, respectively), and the assignment was based on the characteristic $^{13}$C-chemical shifts.

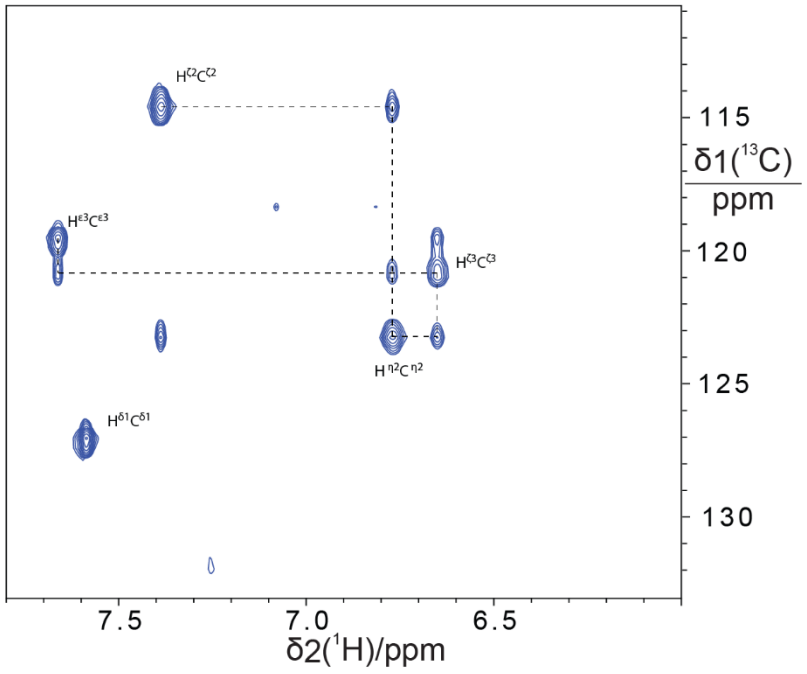


**Figure S7.** $^{13}$C-HSQC with TOCSY relay (20 ms mixing time) for the assignment of the tryptophan indole protons in GB1.

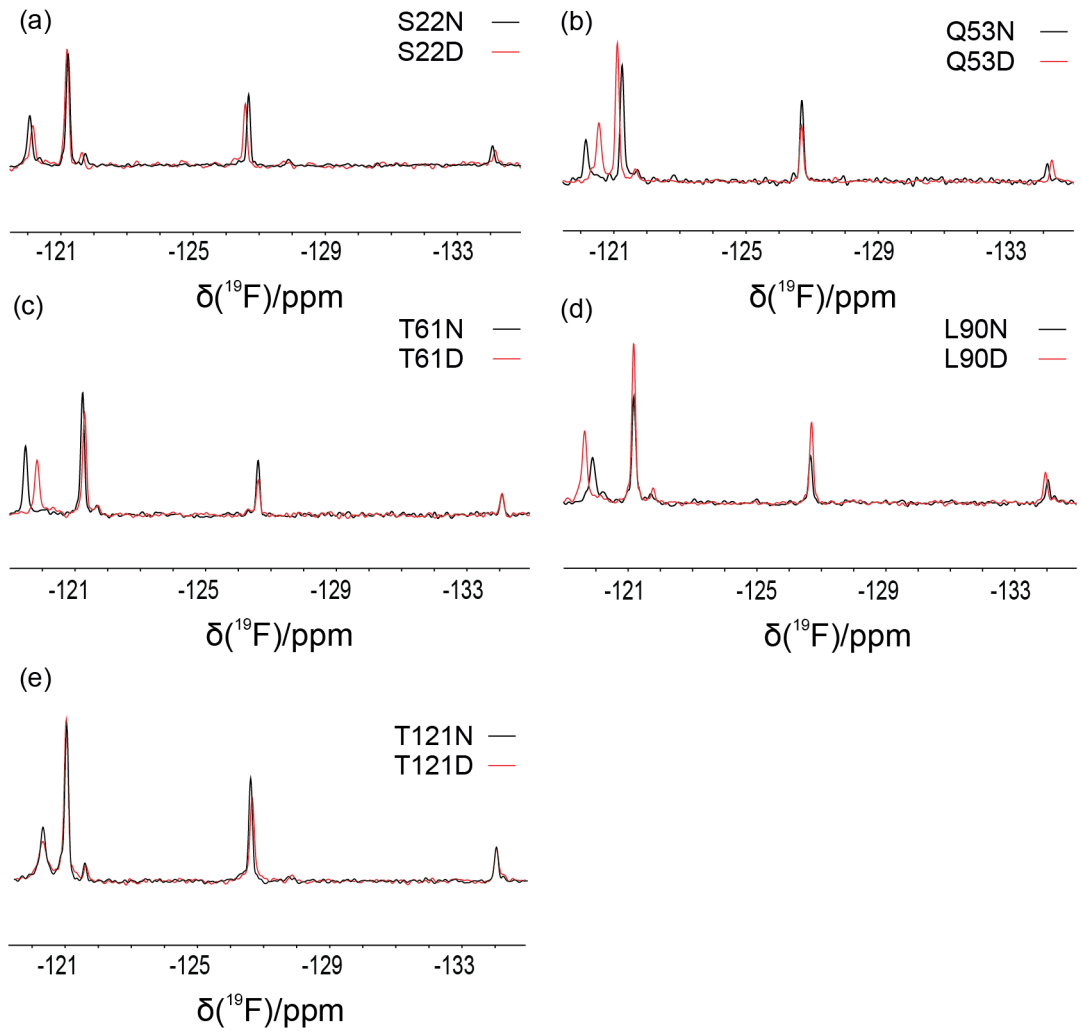


**Figure S8.** 1D $^{19}$F NMR spectra of 4FW, 5FW, 6FW, and 7FW in different mutants of the NT* domain. (a) S22 D/N, (b) Q53 D/N, (c) T61 D/N, (d) L90 D/N, (e) T121 D/N.

**Table S1.** $^{19}$F chemical shift changes in response to Asp/Asn switches in the NT* domain.[a]

| | Δδ□□F)/ppm | | | |
|---|---|---|---|---|
| Mutation sites | 4FW | 5FW | 6FW | 7FW |
| S22 D/N | 0.10 | -0.10 | -0.40 | 0.07 |
| Q53 D/N | 0.39 | 0.00 | -0.14 | 0.13 |
| T61 D/N | 0.35 | 0.00 | 0.06 | 0.00 |
| L90 D/N | -0.25 | 0.04 | -0.01 | -0.07 |
| T121 D/N | 0.00 | 0.04 | -0.01 | 0.00 |

[a] Data of Figure 4a. The chemical shift differences Δδ□□F) are calculated as the chemical shift observed for the protein with Asp minus the chemical shift of the protein with Asn.

**Table S2.** $^{19}F$ chemical shift changes in response to mutations to Asp or Asn in the NT* domain.[a]

| | Δδ□□F)/ppm | | | |
|---|---|---|---|---|
| mutations | 4FW | 5FW | 6FW | 7FW |
| S22N | -0.07 | 0.00 | -0.03 | 0.07 |
| S22D | -0.16 | 0.10 | 0.00 | -0.01 |
| Q52N | -0.17 | -0.01 | -0.07 | 0.01 |
| Q53D | -0.55 | 0.00 | 0.08 | -0.12 |
| T61N | 0.50 | 0.07 | -0.05 | 0.06 |
| T61D | 0.15 | 0.07 | -0.10 | 0.06 |
| L90N | 0.09 | 0.02 | 0.00 | 0.10 |
| L90D | 0.34 | 0.00 | 0.01 | 0.19 |
| T121N | -0.34 | 0.07 | 0.14 | 0.09 |
| T121D | -0.34 | 0.03 | 0.15 | 0.09 |

[a] Data of Figure 4b. The chemical shift differences Δδ□□F) are calculated as the chemical shift observed for the protein mutant with Asp or Asn minus the chemical shift of the wild-type protein.

**Table S3.** $^{1}$H chemical shift changes of tryptophan ring protons in response to mutations to Asp or Asn in the NT* domain.[a]

| | Δδ(¹H)/ppm | | | |
|---|---|---|---|---|
| mutations | H4 | H5 | H6 | H7 |
| S22N | 0.02 | 0.02 | 0.01 | 0.00 |
| S22D | 0.01 | 0.01 | 0.02 | -0.02 |
| Q52N | 0.01 | -0.01 | -0.02 | 0.00 |
| Q53D | 0.02 | -0.04 | -0.10 | -0.16 |
| T61N | 0.00 | 0.00 | 0.01 | 0.03 |
| T61D | 0.00 | 0.00 | 0.01 | 0.02 |
| L90N | 0.01 | 0.02 | -0.03 | -0.04 |
| L90D | 0.01 | 0.02 | -0.06 | -0.03 |
| T121N | 0.01 | 0.01 | -0.01 | -0.05 |
| T121D | 0.00 | 0.01 | 0.00 | -0.03 |

[a] Data of Figure 4d. The chemical shift differences Δδ(¹H) are calculated as the chemical shift observed for the protein mutant with Asp or Asn minus the chemical shift of the wild-type protein.

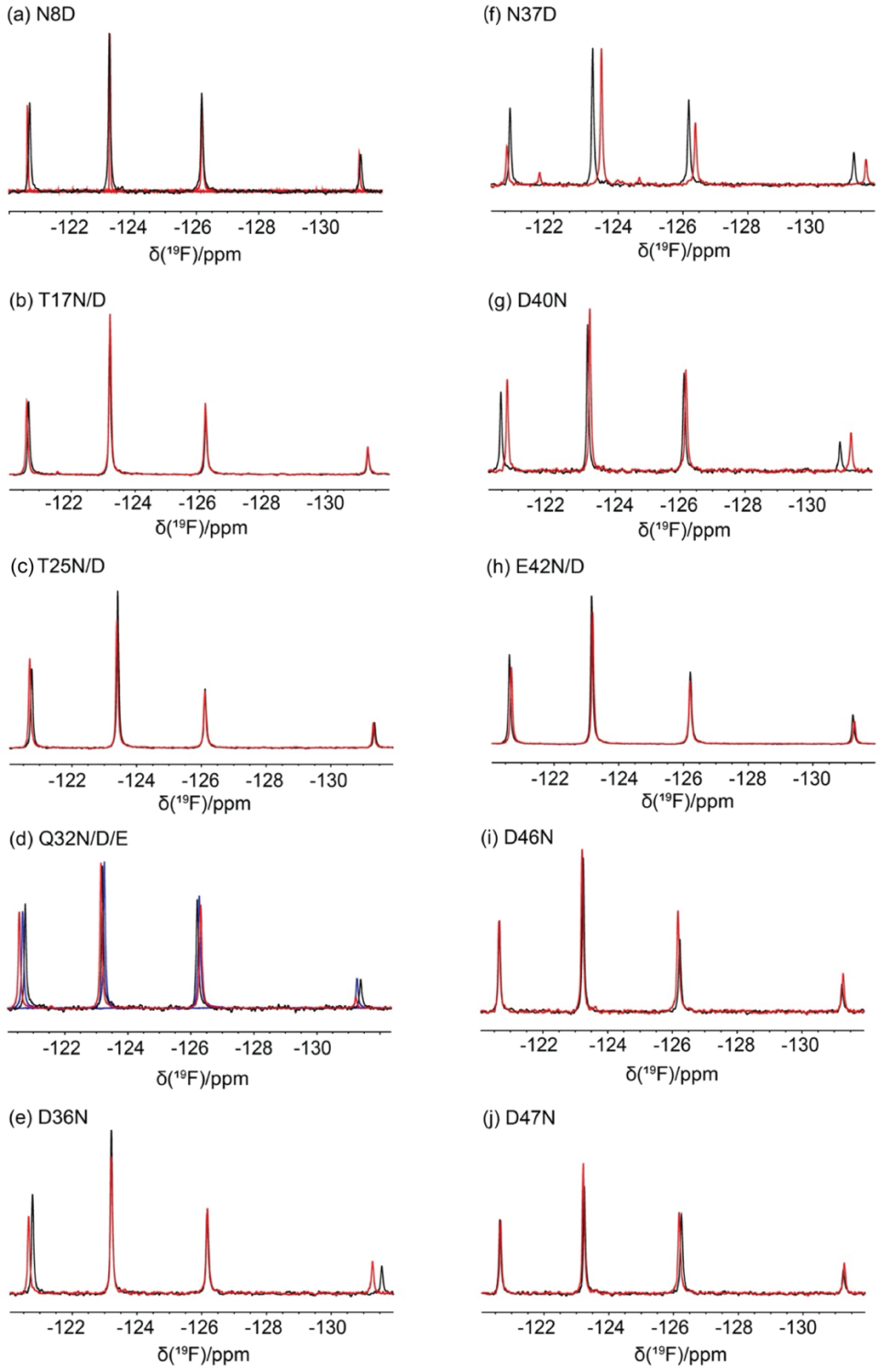


**Figure S9.** 1D $^{19}$F NMR spectra of 4FW, 5FW, 6FW, and 7FW in different GB1 mutants. The spectra of constructs containing Asp, Asn, or Glu in the positions indicated are shown in red, black, or blue, respectively. (a) N8D, (b) T17 D/N, (c) T25 D/N, (d) Q32 D/N/E, (e) D36N, (f) N37 D/N, (g) D40 D/N, (h) E42 D/N, (i) D46 D/N, and (j) D47 D/N.

**Table S4.** $^{19}F$ chemical shift changes in response to Asp/Asn switches in GB1.[a]

| | Δδ(¹⁹F)/ppm | | | |
|---|---|---|---|---|
| mutation sites | 4FW | 5FW | 6FW | 7FW |
| N8 D/N | -0.02 | -0.03 | 0.07 | 0.05 |
| T17 D/N | 0.01 | -0.02 | 0.05 | 0.00 |
| T25 D/N | 0.00 | 0.02 | 0.06 | 0.04 |
| Q32 D/N | -0.11 | 0.05 | 0.20 | 0.16 |
| D36 D/N | -0.01 | 0.00 | 0.12 | 0.30 |
| N37 D/N | -0.21 | -0.28 | 0.10 | -0.40 |
| D40 D/N | -0.06 | -0.07 | -0.20 | -0.34 |
| E42 D/N | 0.02 | -0.03 | -0.06 | -0.05 |
| D46 D/N | 0.06 | 0.03 | -0.02 | -0.04 |
| D47 D/N | 0.07 | 0.03 | -0.02 | -0.03 |

[a] Data of Figure 5a. The chemical shift differences Δδ(¹⁹F) are calculated as the chemical shift observed for the protein with Asp minus the chemical shift of the protein with Asn.

**Table S5.** $^{19}F$ chemical shift changes in response to mutations to Asp or Asn in GB1.[a]

| | Δδ□□F)/ppm | | | |
|---|---|---|---|---|
| mutations | 4FW | 5FW | 6FW | 7FW |
| T17N | -0.02 | 0.01 | -0.02 | 0.02 |
| T17D | -0.01 | -0.01 | 0.03 | 0.03 |
| T25N | 0.07 | -0.20 | -0.09 | -0.06 |
| T25D | 0.06 | -0.19 | -0.05 | -0.04 |
| Q32N | -0.01 | 0.04 | -0.08 | -0.10 |
| Q32D | -0.14 | 0.06 | 0.10 | 0.04 |
| E42N | -0.04 | 0.04 | 0.03 | 0.04 |
| E42D | -0.03 | 0.01 | -0.03 | -0.01 |

[a] Data of Figure 5b and data underpinning Figure 5a. The chemical shift differences Δδ□□F) are calculated as the chemical shift observed for the protein mutant with Asp or Asn minus the chemical shift of the wild-type protein.

**Table S6.** $^{1}$H chemical shift changes of tryptophan ring protons in response to mutations to Asp or Asn in GB1.[a]

| | Δδ□H)/ppm | | | |
|---|---|---|---|---|
| mutations | H4 | H5 | H6 | H7 |
| T17N | 0.00 | 0.01 | 0.00 | 0.00 |
| T17D | 0.01 | 0.01 | 0.00 | 0.00 |
| T25N | 0.00 | -0.01 | 0.00 | 0.00 |
| T25D | 0.00 | 0.00 | 0.00 | 0.00 |
| Q32N | 0.00 | 0.01 | 0.00 | 0.01 |
| Q32D | 0.02 | 0.01 | -0.01 | 0.01 |
| E42N | 0.00 | 0.00 | 0.00 | 0.00 |
| E42D | 0.00 | 0.00 | 0.00 | 0.00 |

[a] Data of Figure 5d and data underpinning Figure 5c. The chemical shift differences Δδ□H) are calculated as the chemical shift observed for the protein mutant with Asp or Asn minus the chemical shift of the wild-type protein.

**Table S7.** Comparison of $^{19}$F chemical shift changes in response to Asp/Asn switches in the NT* domain measured in the presence of 100 and 200 mM NaCl.[a]

| | Δδ(¹⁹F)/ppm | | | |
|---|---|---|---|---|
| mutation sites | 4FW | 5FW | 6FW | 7FW |
| Q53 D/N (high salt) | 0.41 | 0.00 | -0.13 | 0.00 |
| Q53 D/N (low salt) | 0.39 | 0.00 | -0.14 | 0.13 |
| T61 D/N (high salt) | 0.36 | 0.00 | 0.07 | 0.00 |
| T61 D/N (low salt) | 0.35 | 0.00 | 0.06 | 0.00 |
| L90 D/N (high salt) | -0.26 | 0.01 | -0.03 | 0.00 |
| L90 D/N (low salt) | -0.25 | 0.04 | -0.01 | -0.07 |

[a] The chemical shift differences Δδ(¹⁹F) are calculated as the chemical shift observed for the protein with Asp minus the chemical shift of the protein with Asn.

**Table S8.** $^{19}$F chemical shift changes in response to a Glu/Gln switch in GB1 compared with the corresponding Asp/Asn switch.[a]

| | Δδ(¹⁹F)/ppm | | | |
|---|---|---|---|---|
| mutation sites | 4FW | 5FW | 6FW | 7FW |
| Q32 D/N | -0.11 | 0.05 | 0.20 | 0.16 |
| Q32 E/Q | -0.09 | -0.04 | 0.00 | 0.01 |

[a] The chemical shift differences Δδ(¹⁹F) are calculated as the chemical shift observed for the protein with Glu (Asp) minus the chemical shift of the protein with Gln (Asn).

**Table S9.** $^{19}F$ chemical shift changes in response to the Asp/Asn switch in position 32 of wild-type GB1 and GB1 K31M.[a]

| | Δδ□□F)/ppm | | | |
|---|---|---|---|---|
| mutation sites | 4FW | 5FW | 6FW | 7FW |
| WT Q32 D/N | -0.13 | 0.04 | 0.19 | 0.15 |
| K31M Q32 D/N | -0.09 | 0.06 | 0.21 | 0.10 |

[a] The chemical shift differences Δδ□□F) are calculated as the chemical shift observed for the protein with Glu (Asp) minus the chemical shift of the protein with Gln (Asn).

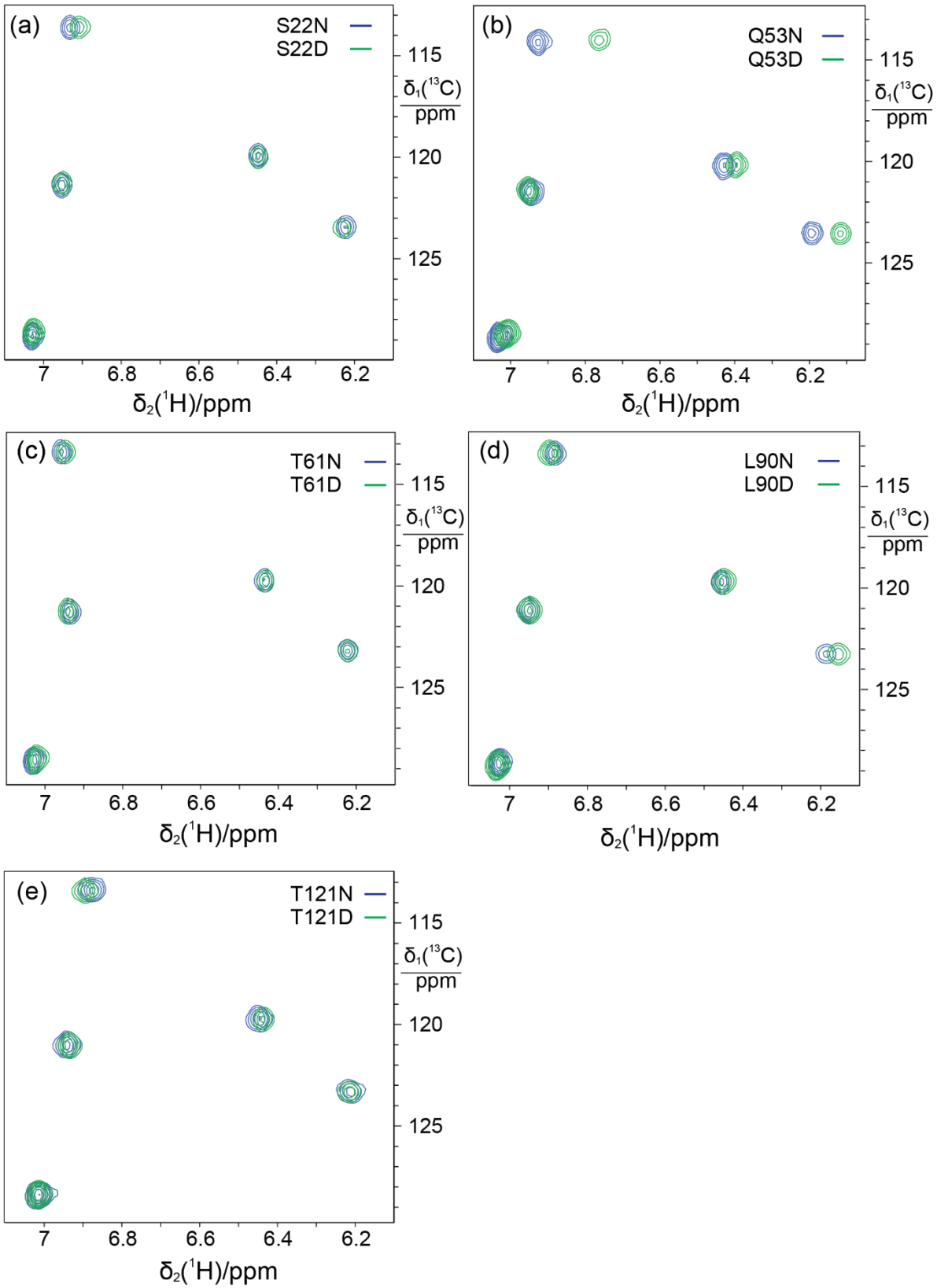


**Figure S10.** $^{13}$C-HSQC spectra of NT* domain mutants made with $^{13}$C/$^{15}$N labeled tryptophan. (a) S22N and S22D overlay. (b) Q53N / Q53D. (c) T61N / T61D. (d) L90N / L90D. (e) T121N / T121D. Asparagine mutant spectra are shown in blue and aspartate is shown as green.

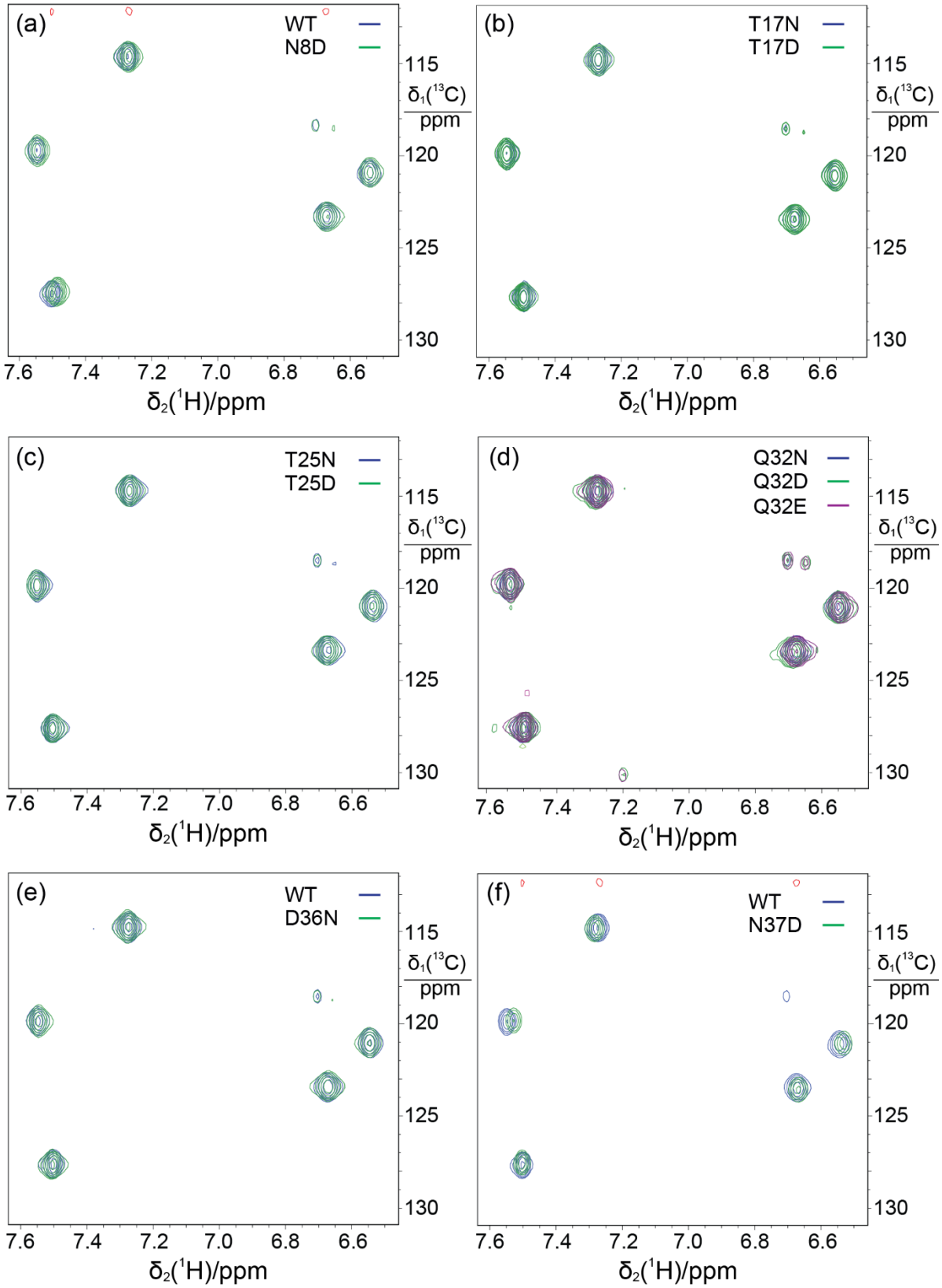
(a)
WT
N8D
(b)
T17N
T17D
(c)
T25N
T25D
(d)
Q32N
Q32D
Q32E
(e)
WT
D36N
(f)
WT
N37D
115
120
125
130
δ1(13C)
ppm
7.6
7.4
7.2
7.0
6.8
6.6
δ2(1H)/ppm

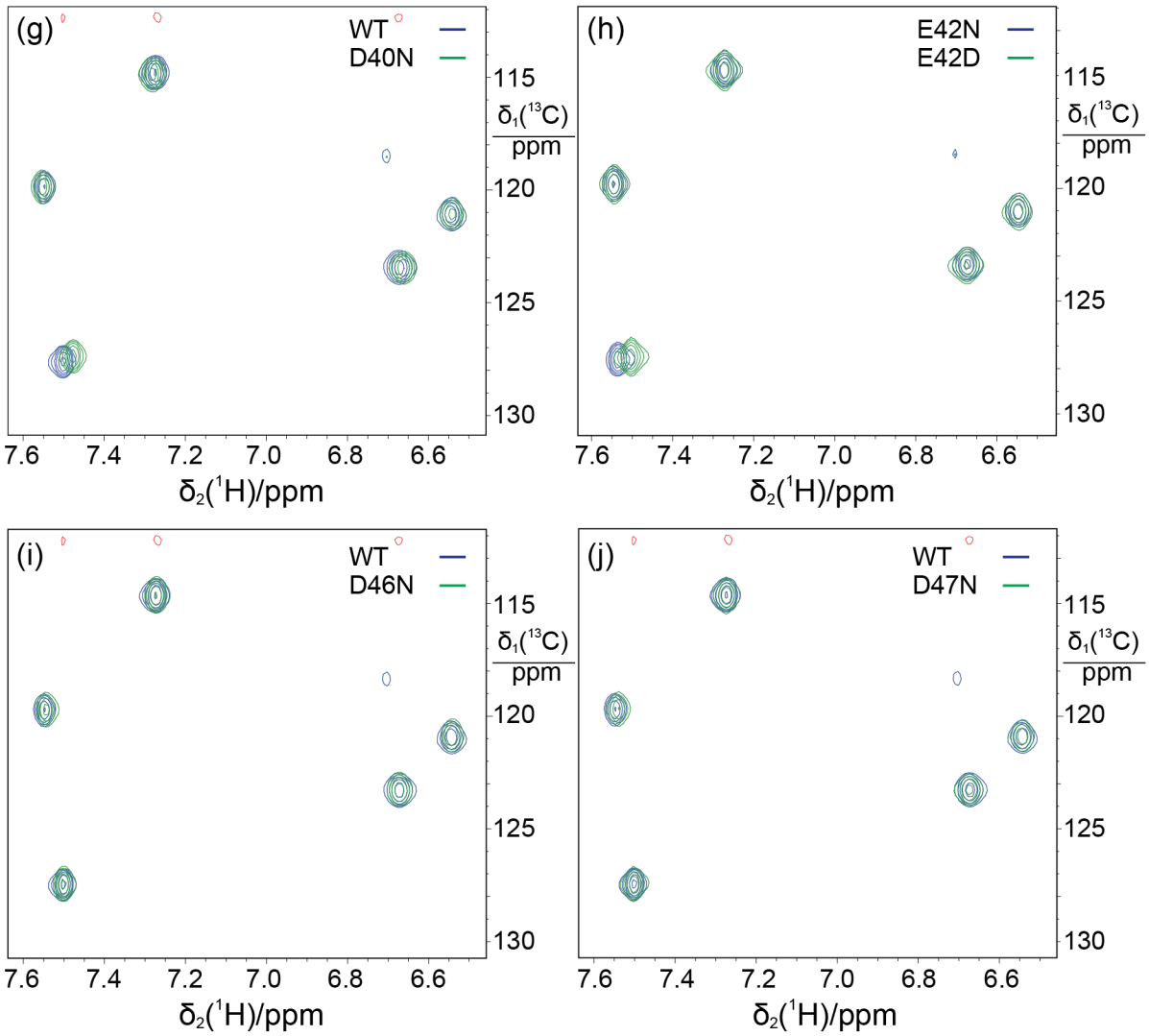


**Figure S11.** $^{13}$C-HSQC spectra of GB1 mutants with $^{13}$C/$^{15}$N-labeled tryptophan. Two (or three) spectra are overlayed in each panel. Color code: Asp - green, Asn – blue, Glu - purple. (a) N8 D/N, (b) T17 D/N, (c) T25 D/N, (d) Q32 D/N and E, (e) D36 D/N, (f) N37 D/N, (g) D40 D/N, (h) E42 D/N, (i) D46 D/N, (j) D47 D/N.

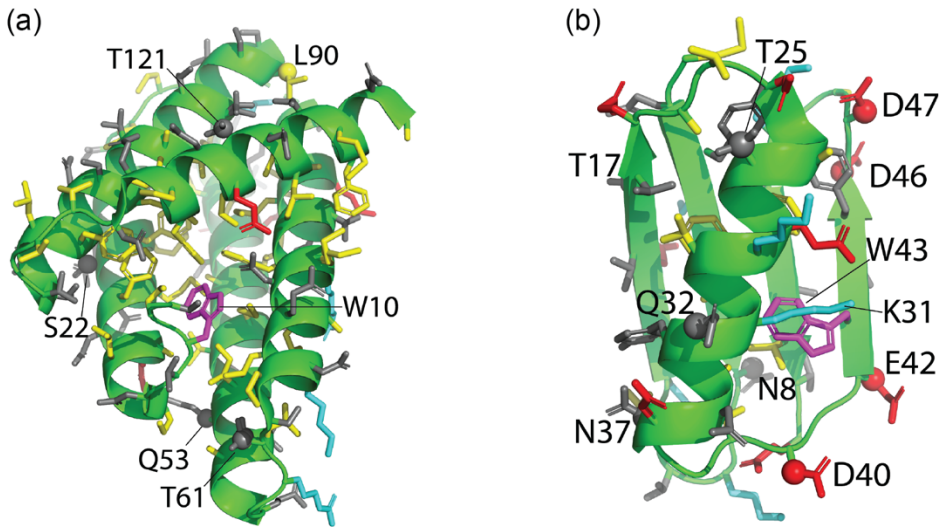


**Figure S12.** Cartoon representations of the crystal structures of the NT* domain and GB1. The structures are shown in the same orientation as in Figures 6 and 7 of the main text, using the same color code except that tryptophan side chains are highlighted in magenta. (a) NT* domain (PDB ID: 4FBS). (b) GB1 (PDB ID: 2QMT).

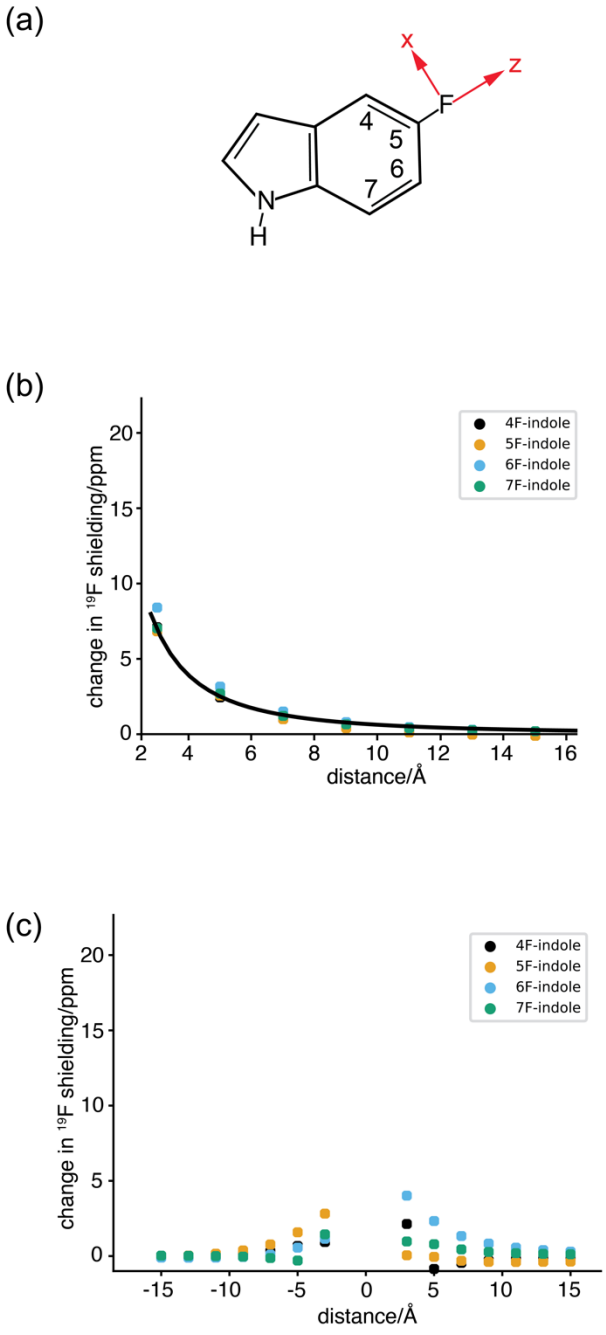


**Figure S13.** Calculated change in $^{19}$F chemical shift due to an electric charge (+0.5) at different distances from the $^{19}$F spin in different fluoroindoles. (a) In the orthonormal coordinate system used, the origin is at the position of the fluorine atom, the z axis points along the C-F bond, the x axis is in the plane of the indole ring system, and the y axis is perpendicular to the plane of the indole ring system. The drawing shows the coordinate axes for 5-fluoroindole. (b) Change in $^{19}$F shielding along the y axis. The effect is about 3-fold smaller than along the z axis (Figure 9). The black curve corresponds to a quadratic decay. (c) Change in $^{19}$F shielding along the x axis.

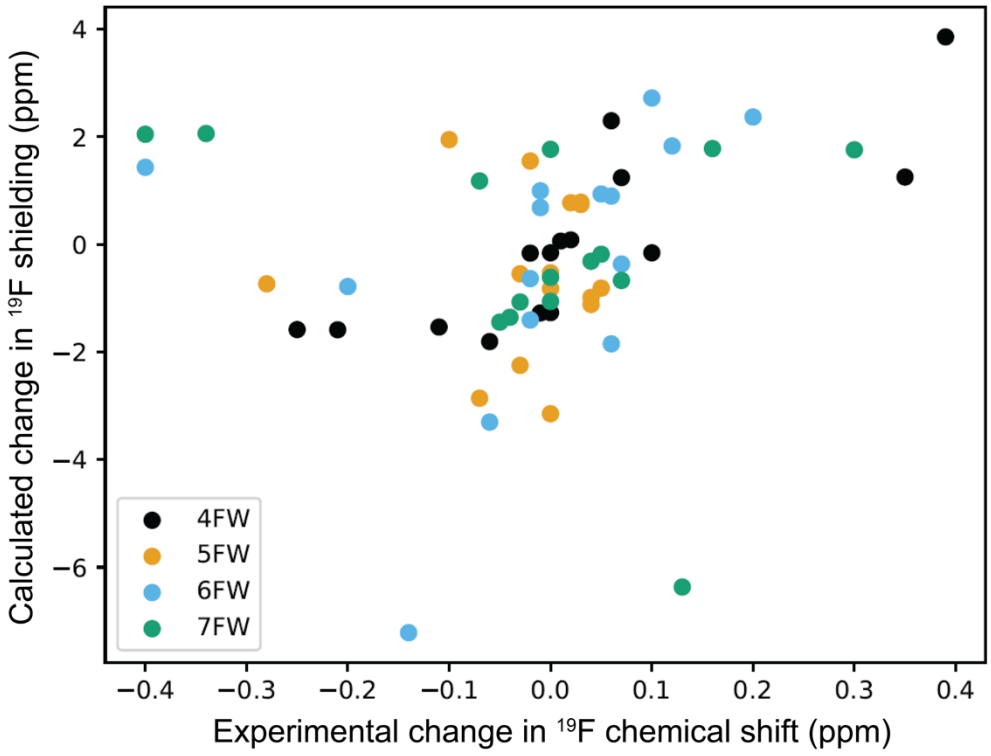


**Figure S14.** Correlation of predicted and experimental $^{19}$F chemical shift changes effected by Asp/Asn switches in GB1 and the NT* domain. DFT calculations were performed on 4F-indole, 5F-indole, 6F-indole, and 7F-indole in vacuum with a point charge of +0.5 positioned on a regular grid with 2 Å spacing in all three dimensions. To calculate the charge effect on the $^{19}$F shielding, the crystal structures of the proteins (GB1: PDB ID 2QMT; NT* domain: PDB ID 4FBS) were translated and rotated to superimpose the indole moieties of the fluorotryptophans on the requisite grid, and the $^{19}$F shielding values at the locations of the Asp/Asn switches were linearly interpolated. The experimental data are given in Tables S1 and S4.